Substrate Finishing and Niobium Content Effects on the High Temperature Corrosion Resistance in Steam Atmosphere of CrN/NbN Superlattice coatings Deposited by PVD-HIPIMS

Andrea Illana[a], Sonia Mato[a], Arutiun Ehiasarian[b], Yashodhan Purandare[b], María Isabel Lasanta[a], María Teresa de Miguel[a], Papken Hovsepian[b], Francisco Javier Pérez-Trujillo[a]

[a]*Grupo de Ingeniería de Superficies y Materiales Nanoestructurados. Universidad Complutense de Madrid. 28040 Madrid, SPAIN*
[b]*Materials and Engineering Research Institute, Sheffield Hallam University. Sheffield S1 1WB, UNITED KINGDOM*

ailla01@ucm.es; msmatodi@ucm.es; a.ehiasarian@shu.ac.uk; y.purandare@shu.ac.uk; milasant@ucm.es; mtdmiguel@ucm.es; p.hovsepian@shu.ac.uk; fjperez@ucm.es

Abstract. The main objective of this work was to evaluate the oxidation resistance of three PVD-HIPIMS CrN/NbN coatings, studying the effect of the surface finishing of the substrate and the role of niobium content into the coating composition. CrN/NbN nano-multilayered films on P92 steel were tested at 650°C in pure steam atmosphere. The mass gain was measured at fixed intervals to study their oxidation kinetics. The morphology and thickness of nanoscales were measured by transmission electron microscopy (TEM). Characterization of coatings before and after the thermal treatment was performed by scanning electron microscopy-energy with facilities of dispersive X-ray spectroscopy (SEM–EDX) and X-ray diffraction (XRD). All coatings improved the oxidation resistance of the substrate material, but the best behaviour was exhibited by the CrN/NbN with the high niobium (Nb) content and deposited on the substrate with the finest surface finishing.

Keywords: High temperature, Steam oxidation, CrN/NbN coating, Surface finishing.

INTRODUCTION

Environmental restrictions entail an increase in thermal efficiency of conversion processes in steam turbines of electric generation power plants. In this way, a reduction of the fuel consumption can be achieved as well as of pollutant gases emissions [1]. To achieve that goal, the use of more expensive materials which are able to resist ultra-supercritical conditions (USC) at 625-650°C is demanded [2]. The new generation of 9-10% Cr steels owns enough mechanical properties [3] to be considered as candidate to manufacture turbine components, but they exhibit a limited oxidation resistance at USC in steam atmosphere [4]. In the last decades, protective coatings have been explored in order to retard interdiffusion phenomena which take place at that temperature range, achieving a prolongation of the service life of base materials [5-7].

Chromium nitride films have been extensively applied by physical vapour deposition (PVD) on mechanical components, because of their excellent tribological characteristics [8] and the ability of formation of a layer of protective chromia on the surface which confers corrosion resistance at high temperature [9]. In order to improve their behaviour, additional elements have been included in their composition such as Al, Ti, Nb and rare earths as Y or Zr [10-12]. Following other approach different arrangements of the coating multilayers have been also tested exploring the effect of alternating layers with thickness and composition variations [13-15].

Coatings with a CrN/NbN superlattice consisting of alternating layers of CrN and NbN with a nanometric thickness in at least one of the layers have shown interesting properties [16]. On one hand CrN provides good wear resistance. On the other hand NbN has a high chemical stability and improves wet corrosion resistance based on the formation of niobium oxide (Nb_2O_5) [16, 17]. The high number of interfaces related with the periodicity of the layers limits the propagation of cracks imparting CrN/NbN coating excellent tribo-corrosion resistance [13, 18]. However, the performance of the coating will depend also on the defects developed in the growth of the coating depending on the PVD technique used [19]. For example, during arc evaporation deposition or during arc etching in arc bond sputtering (ABS) process, spherical droplets (macro-defects) are produced which compromise the coating effectiveness generating a galvanic couple between the defect and the coating matrix or stresses accumulation at the droplet-coating interface [20]. Also porosity and under-dense structures, which have been reported to be present in coatings deposited by sputtering techniques, can compromise mechanical and corrosion properties to a large extent [20-23]. CrN/NbN coatings deposited by high power impulse magnetron sputtering (HIPIMS) technique have shown to overcome all these drawbacks, retaining the good adhesion produced by arc techniques, as well as the smooth dense structures produced by sputtering techniques [21-23].

The capability of CrN/NbN coatings with droplet defects produced by arc etching followed by unbalanced magnetron sputtered (UBM) deposition in resisting oxidation [24], and that of coatings with superior microstructure produced by combined HIPIMS-UBM technique in resisting room temperature wet corrosion and tribo-corrosion has been documented earlier [23, 24]. The main objective of this work was the evaluation of the oxidation behaviour of defect free (droplet free and dense structures) CrN/NbN coatings produced by HIPIMS technique on P92 steel at high temperature and wet corrosive conditions. Additionally, the oxidation resistance enhancement provided by the presence of niobium in the coatings, through the development of oxide scales such NbO and Nb_2O_5 is under discussion. However, some authors have suggested that if these scales present low porosity and remain intact at high temperatures (do not develop cracks or porosity) [25-29] their oxidation resistance capability can be improved. Therefore a secondary objective was to analyse the effect of Nb concentration on the oxidation resistance of the CrN/NbN multilayer coatings. To achieve this goal a coating with sublayers with higher atomic % of Nb has been deposited and tested. Further, the effect of the surface finishing of the substrate before the coating deposition has also been explored.

EXPERIMENTAL PROCEDURES

Materials: substrate and coatings

The coatings were deposited on P92 ferritic-martensitic steel, which chemical composition is indicated in Table 1. Coupons of 20x10x3 mm were cut from a sheet and grounded by means of a grinding wheel of Al_2O_3 abrasive with vitrified bond (#46). The surface of selected specimens was further grounded with SiC grit paper up to #1000. Prior to deposition each specimen was cleaned in an ultrasonic bath with aqueous alkali solution, rinsed with deionized water, and subsequently dried in a vacuum drier.

TABLE 1. Composition of P92 steel used as substrate in this work (in wt.%).

Fe	Cr	W	Mn	Mo	Si	Ni	V	C	Nb	N	Al	B
Bal.	9.0	1.75	0.45	0.45	0.25	0.2	0.2	0.1	0.06	0.05	0.02	0.004

CrN/NbN multilayered coatings were deposited in an industrial sized PVD machine (HTC 1000-4, Hauzer Techno Coatings, Europe B.V., Venlo, The Netherlands) which has four cathodes capable of working in HIPIMS or UBM mode. For this study coatings were produced on samples which were placed on a rotating substrate table capable of achieving three fold rotation for uniform coverage of all the surfaces. While rotating the samples traverse in front of pure metallic targets which are sputtered; in this case two Cr and two Nb (99.9% purity) targets placed diagonally opposite to each other. For deposition, one target of Cr and Nb were operated in HIPIMS mode (power supplies from Hüttinger Elektronik Sp. z o.o., Warsaw, Poland) whereas the remaining two were operated in UBM mode. The details of the machine, arrangement of the targets and the coating scheme can be found in another publication [23]. The coating process was carried out, in three steps: HIPIMS pre-treatment to etch the substrate surface, followed by a reactive deposition ($Ar+N_2$ atmosphere) of a CrN base layer to promote a better adhesion between the substrate and the coating, and finally deposition of alternating nanoscale layers of CrN and NbN to form a CrN/NbN multilayers coating. The deposition has been carried out at 400°C and at a bias voltage of -65V.

Stoichiometry of a PVD deposited coatings depends on a number of parameters. The most influential are the partial pressures of processes gasses (in this case Ar/N_2) and relative powers on the cathodes. Thus for a CrN/NbN multilayer coating deposited at a fixed total chamber pressure, relative atomic percentage of Cr in CrN as well as Nb in NbN (N/Me and Cr/Nb ratios) will depend on the powers applied on the cathodes containing Cr and Nb targets respectively.

In order to study the effective of Nb on the oxidation resistance, Nb content in the coatings was increased by increasing the power on the Nb cathode during multilayer deposition step. Thus two types of multilayer CrN/NbN coatings were created, however CrN base layer was kept the same for all the 3 coatings (N/Cr = 1). Table 2 gives

difference in the chemical composition and change in the bi-layer thickness of these two types of coatings. Thus in this study three types of specimens were tested: CrN/NbN with lower Nb content and CrN/NbN with higher Nb content on P92 with coarse surface substrate preparation and CrN/NbN with higher Nb on P92 with fine surface substrate preparation. Table 2 also shows a summary of substrate preparation before the deposition.

TABLE 2. EDX chemical composition (in at. %) and bi-layer thickness of coatings and specifications about substrate preparation.

Coating	Chemical composition			Bi-layer thickness	Substrate preparation
	N_2	Cr	Nb	(nm)	
Low Nb-CrN/NbN #46	57.96	29.87	12.17	2.9	Mechanical grinding (ϕ=370 μm)
High Nb- CrN/NbN #46	51.38	26.17	22.45	1.9	
High Nb-CrN/NbN #1000	51.38	26.17	22.45	1.9	Grit paper (ϕ=15.3 μm)

Steam Oxidation Tests

P92 and coated samples were oxidized at 650ºC in 100% steam atmosphere in order to simulate the operation conditions of supercritical turbines. The isothermal oxidation test was carried out in two connected tubular horizontal furnaces. In the first furnace, the vapour was generated from de-oxygenated water which was recirculated by a condenser system, and in the second, the specimens were oxidized. A detailed description of the experimental set up was shown in previous works [30]. N_2 constant flow was injected into the close circuit to prevent the samples oxidation while the furnace was cooled down to room temperature or heated up to the working temperature. Three specimens of each coating were oxidized, for the purpose of ensuring the reproducibility of the results. The specimens were removed from the furnace at different intervals in order to evaluate their mass gain variation with time by means of a five decimal balance, to determine and compare the oxidation kinetics of each coating.

Characterization Techniques

The microstructure of the CrN/NbN multilayer coatings was explored using a Philips CM20 STEM transmission electron microscopy (TEM) whereas low angle XRD technique was used to calculate the bi-layer thickness. In order to analyse the morphology and chemical composition of as-deposited and oxidized coated samples, their surfaces and cross-sections were observed by scanning electron microscopy with energy dispersive X-ray spectroscopy facilities (SEM–EDX) in a JEOL JSM-820 at 20 kV and 15 mm of working distance. For the cross-section preparation the specimens were embedded in phenolic resin and grounded up to #2400 SiC grit paper. After, the samples were cleaned with distilled water and 2-propanol solution and, finally, dried in warm air. Crystalline phases were determined by X-ray diffraction (XRD) in a PANalytical X'Pert PRO MRD diffractometer and the help of the Joint Committee on Powder Diffraction and Standards (JCPDS) databases. Bragg-Brentano (θ-2θ) and gracing angle

(θ=0.5º) modes were employed at 45 kV and 40 mA ($K_{\alpha 1\ Cu}$), in the scan range 10-100º (2θ). Bragg-Brentano geometry allows elucidating the preferential plans parallel to the sample surface. Besides, the use of gracing angle mode reduces the substrate signal and increases the detected signal of preferential plans perpendicular to the sample surface. Comparison of both results facilitates the diffraction peaks assignation.

RESULTS AND DISCUSSION

As-deposited coatings

Fig. 1 exhibits the surface morphology of the coatings before the oxidation test. As observed, the surfaces show some defects (average diameters of 5 μm), typical of PVD techniques, generated due to contamination from the surrounding chamber walls and fixtures [30]. The coatings deposited on the substrates with coarse grinding (Fig. 1a-b) showed parallel lines due to the rough and unidirectional surface finishing. Deposited CrN/NbN coating, being thin in nature follows the topography very closely thereby retaining the original surface finish; in this case the rough and unidirectional groves. The coatings deposited on the substrates grounded up to #1000 (Fig. 1c) appeared smoother without prominent groves and with uniform coating distribution all over the surface. This surface being smoother prominently shows the superficial contamination defects as compared to the rough grooved sample.

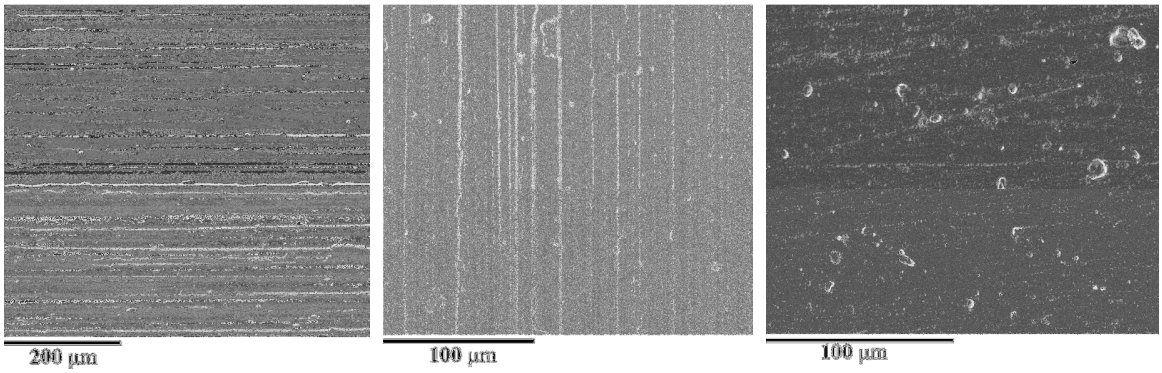

(a) (b) (c)

FIGURE 1. Superficial SEM micrographs of as-deposited coatings (a) low Nb-CrN/NbN #46, (b) high Nb-CrN/NbN #46 and (c) high Nb-CrN/NbN #1000.

XRD analysis in Bragg-Brentano geometry of the as-deposited coatings is shown in Fig. 2. The three coatings, independent of surface finishing of substrate and the Nb content, confirmed the presence of diffraction peaks corresponding to the coating CrN/NbN, whose preferential planes are indicated in Fig. 2a.

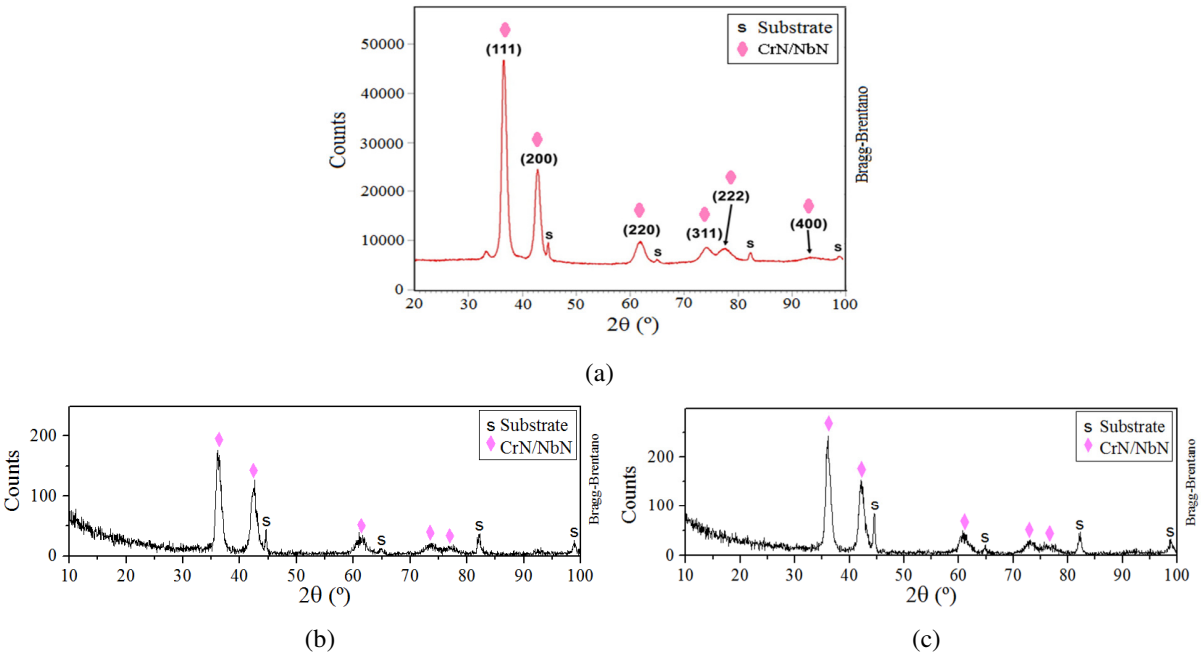

FIGURE 2. XRD analysis of as-deposited coatings (a) low Nb-CrN/NbN #46, (b) high Nb-CrN/NbN #46 and (c) high Nb-CrN/NbN #1000.

Fig. 3 shows the low Nb-CrN/NbN coating structure examined by TEM. The coating consists of a number of individual nanoscale layers of CrN and NbN stack in an alternative repetitive order to form a nanoscale multilayer coating. Owing to the numerous interfaces between the individual nitride layers of Cr and Nb along with their inherent wear resistance and electrochemical nobility, the CrN/NbN multilayer enjoys a superior wear and corrosion resistance as compared to monolithic coatings [13, 23]. The thickness of consecutive layers of CrN and NbN is defined as the bi-layer thickness. Low angle XRD studies revealed that the CrN/NbN coatings with lower atomic % Nb had a bi-layer thickness of 2.9 nm whereas with higher atomic % Nb had a bi-layer thickness of 1.9 nm.

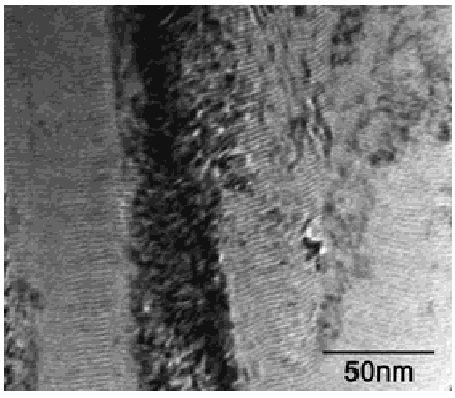

FIGURE 3. TEM micrograph of as-deposited low Nb-CrN/NbN coating.

In Fig. 4, two representative cross-sections of the high Nb-CrN/NbN coatings but different substrate surface finishing are compared. PVD coating techniques is a line of sight process i.e. in order to coat a substrate; the surface should face the incoming flux of the coating material. Any shadowed area will be depleted of the coating flux and can give rise to defective microstructure such as under-dense structures, porosity or weakened bonding with the surrounding material. The highly ionised plasmas in HIPIMS technique, which has a higher ratio of metal and gas ions to neutral as compared to other sputtering techniques [13] helps to overcome this problem. The highly ionised flux, under the influence of a suitable bias voltage, helps to improve ad-atom mobility, thereby improving the specimen coverage.

Fig. 4a shows such an example of a heavily shadowed area; in this case area under the grove caused by the grinding step of substrate preparation. The benefit of using HIPIMS technique is evident. Even though very rough and heavily shadowed, the coating coverage appears substantial, homogeneous and well adhered to the substrate; especially as compared to normal sputtering which would have struggled to achieve such an extensive coverage. However in this case, the coating still shows some discontinuity near the boundary of the grove (black area in Fig. 4a). The current set of coatings was deposited with a bias voltage of -65 V. It will be interesting to see if higher bias voltages can completely resolve this issue.

In the case of smooth substrates (#1000 grounded) the issue of shadowing is absent and the coating appears to be very dense, without discontinuity and much uniform and strongly adhered to the substrate (Fig. 4b). The CrN/NbN coating with coarse grinding showed an average thickness of 10 μm whereas smooth substrates thickness was slightly lower, around 6 μm.

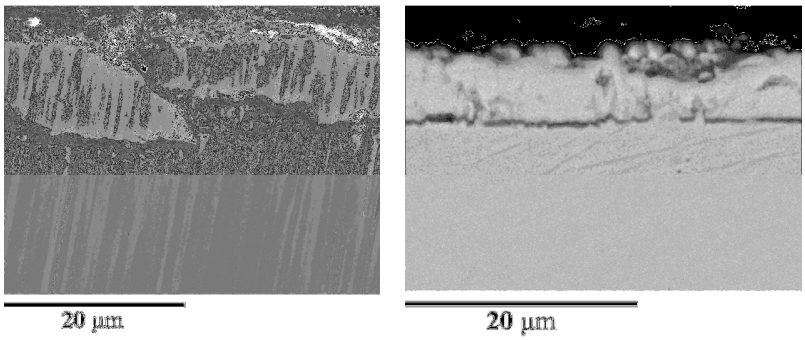

(a) (b)

FIGURE 4. Cross-sectional SEM micrographs of as-deposited CrN/NbN coatings with high Nb content on P92 surfaces prepared up to (a) #46 and (b) #1000.

Oxidation Kinetics

Fig. 5 displays the gravimetric curves of the coatings and substrate material recorded during the oxidation tests at 650ºC in 100% steam atmosphere. The mass gain per unit area was calculated as the average of weight measures of

the three specimens of each specimen when they were removed from the furnace at fixed times. The P92 oxidation rate was several orders of magnitude higher to that measured for the coatings. This behaviour is related to the formation of thick and non-protective scales of iron and iron-chromium oxides [4]. Oxidation kinetics of the coating followed a similar tendency to that of P92 steel which traced a parabolic curve after completion of the oxidation test at 2000 h.

Among the CrN/NbN coatings, that with a high Nb content and a coarse finishing of the substrate surface disclosed the highest oxidation rate (average mass gain of 0.40 mg/cm^2 after 2000 h), which it was expected regarding the discontinuities found in the as-deposited coating observed in the Fig. 4a. After 2000 h of oxidation, the coating with the substrate surface grounded up to #1000 exhibited a lower mass gain per unit area of 0.23 mg/cm^2. Therefore, attending to this, the preparation of substrate surface before the coating deposition by PVD-HIPIMS techniques seems to play an important role on the oxidation rate at the studied experimental conditions.

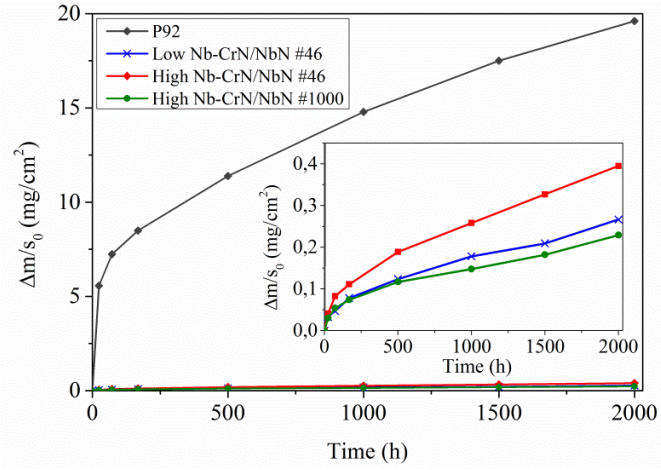

FIGURE 5. Mass change per unit area versus time of the substrate P92 steel and CrN/NbN coatings tested at 650ºC in 100% steam atmosphere and magnification of the measured evolution of coated samples.

Oxidized coatings

After oxidation tests, the coatings showed bright nodules on the surface, as it is observed in Fig. 6. Their average diameters have a range of 5 μm, but the multilayers with high Nb content deposited on the substrates with coarse grinding had also some nodules of larger size (>100 μm). In order to clarify the nature of these defects the CrN/NbN coating and CrN/NbN with high Nb content, have been analysed by SEM-EDX to obtain their semi-quantitative composition (see values of Analysis 1 in Table 3). The small nodules exhibited similar composition, with Cr and O in high proportion indicating the presence of a chromium oxide with small amounts of Nb. However, nodules of higher size had elevated amounts of Fe indicating that diffusion of species from the substrate has occurred.

Extensive needle-like corrosion products were observed all over the surface in the coatings with the coarse substrate surface finishing after 2000 h of oxidation. Compositional analysis of surface, shown in Analysis 2 in Table 3, revealed the presence of similar oxides to those found in the former coating. In addition, microcracks extending across the entire surface were found in the coatings with high content of Nb.

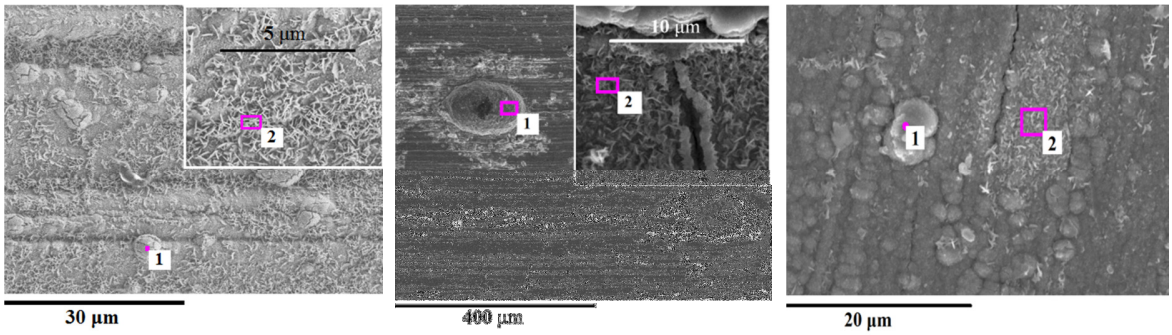

(a) (b) (c)

FIGURE 6. Superficial SEM micrographs of oxidized coatings at 650ºC in 100% steam atmosphere, after 2000 h: (a) low Nb-CrN/NbN #46, (b) high Nb-CrN/NbN #1000 and (c) high Nb-CrN/NbN #1000.

TABLE 3. Composition of defects observed on the surface of oxidized coatings by EDX (in at. %).

Coating	Analysis 1				Analysis 2			
	Fe	Cr	Nb	O	Fe	Cr	Nb	O
Low Nb-CrN/NbN #46	-	22.91	6.08	71.01	-	21.90	5.45	72.65
High Nb-CrN/NbN #46	77.01	1.50	-	21.49	-	24.22	7.47	68.30
High Nb-CrN/NbN #1000	-	32.75	13.29	53.97	-	29.96	12.47	57.57

The SEM micrographs of the cross-sections of the oxidized coatings are displayed in the Fig. 7. Even after 2000 h at experimental conditions, the low Nb coatings (Fig 7a), deposited on P92 surface grounded up to #46, conserved the homogenous thickness and coating-substrate interface even though uneven in nature (due to the coarse finishing of the substrate surface). In Fig 7b a large size oxide nodule (composition rich in Fe from the underlying substrate) is seen directly above the part of the intact coating which is in between two discontinuities. However no such large size oxide nodules, Fig 7c, are seen in the case of high Nb-CrN/NbN coating on smooth substrates (#1000 finish substrates). Thus it seems that the discontinuities, as previously observed in as-deposited high Nb-CrN/NbN coatings on coarse substrate surface, facilitate the growth of these oxide nodules on the surface of the coating.

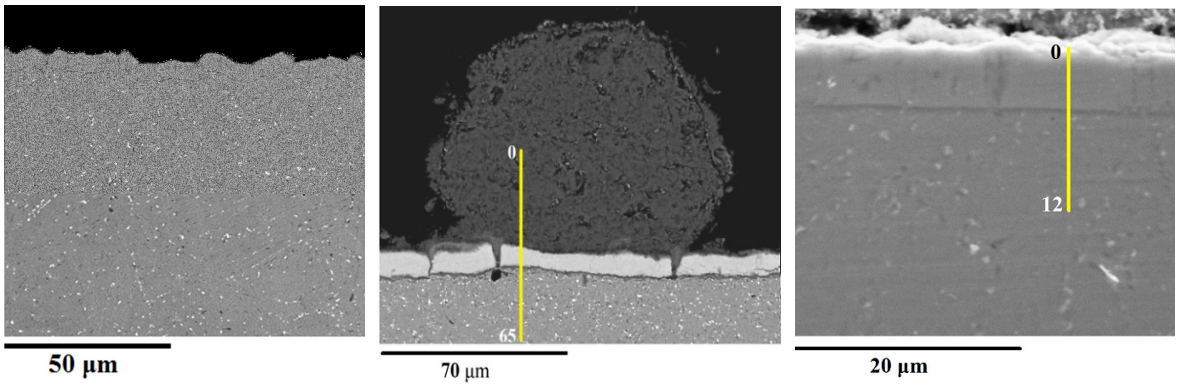

(a) (b) (c)

FIGURE 7. Cross-sectional SEM micrographs of oxidized coatings at 650ºC in 100% steam atmosphere, after 2000 h: (a) low Nb-CrN/NbN #46, (b) high Nb-CrN/NbN #46 and (c) high Nb-CrN/NbN #1000.

In Fig. 8a, EDX line scan analysis verified elevated concentrations of Fe and O in the nodules (about 30 microns in size), but no O was measured through the coating thickness. Consequently, the mass gain measured during oxidation of this coating can be related with the oxidation of the substrate due to pre-existing defects caused probably due to rough topography of the substrate. This is confirmed by the results showed in the Fig. 7b, since the EDX analysis of the coatings deposited on fine grinded substrates, after 2000 h of oxidation confirmed the absence of Fe and O in the coating thickness. Therefore, in agreement with the low mass gain measured for the high Nb-CrN/NbN coating grinded up to #1000, this coating maintained its protective capabilities after 2000 h of oxidation at the selected experimental conditions.

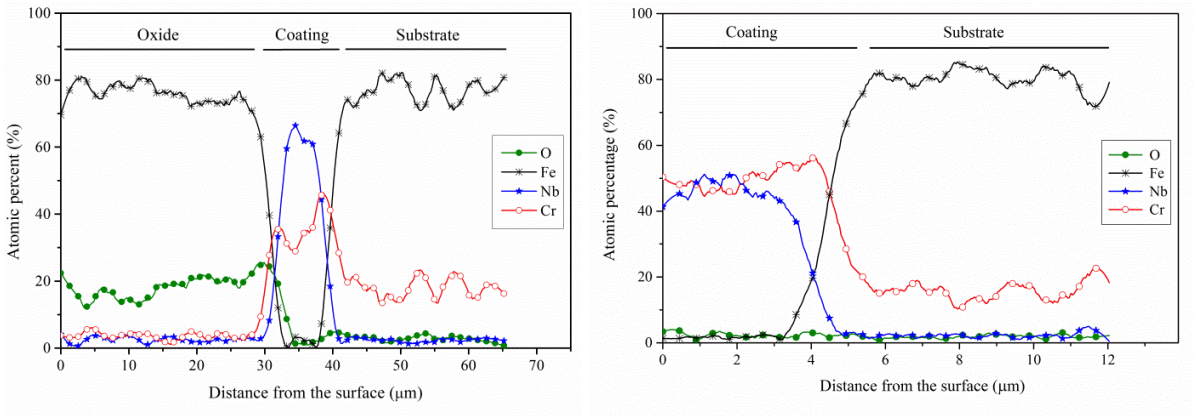

(a) (b)

FIGURE 8. Cross-sectional EDX analysis of oxidized coatings with high Nb content at 650ºC in 100% steam atmosphere after 2000 h, deposited on P92 surfaces prepared up to (a) #46 and (b) #1000.

XRD analysis in Bragg-Brentano geometry performed on the low Nb-CrN/NbN coatings deposited on substrates grinded up to #46, after 2000 h oxidation (Fig. 9a) showed diffraction peaks related to the original coating as well as to Cr and Nb oxides. The presence of diffraction peaks associated to iron oxide also indicates the interdiffusion of Fe species throughout the coating which seems to be possible through the defects generated in the coatings due to contamination, as SEM and XRD analysis confirms the coating to be intact. Figure 9b and figure 9c show the XRD results on coatings with high Nb content where the lower diffractogram represent the Bragg-Brentano results whereas the upper diffractogram represents the grazing angle results. Grazing angle XRD results in figure 9b (high Nb-CrN/NbN #46) confirm the presence of scales made up of oxides of Fe, Cr and Nb which are thick since the scans do not pick any coating peaks. However these coating peaks are visible in the Bragg-Brentano scan which clearly indicates the presence of the coating underneath these scales.

Similarly, grazing angle XRD results for the high Nb-CrN/NbN coating grinded up to #1000, after 2000 h of oxidation (Fig 9c), shows the presence of comparatively thinner chromium oxide (Cr_2O_3) scales and few peaks from the coating underneath. Comparing results from both grazing and Bragg-Brentano scans suggests no interdiffusion of Fe or O since the diffractions peaks are related mainly to the coating and Cr oxide. The presence of diffraction peaks of CrN/NbN phase in oxidized CrN/NbN coatings (irrespective of the Nb content and surface finish) confirmed their stability at the oxidation test conditions.

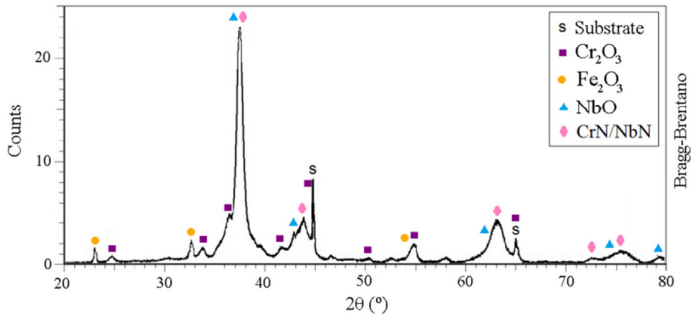

(a)

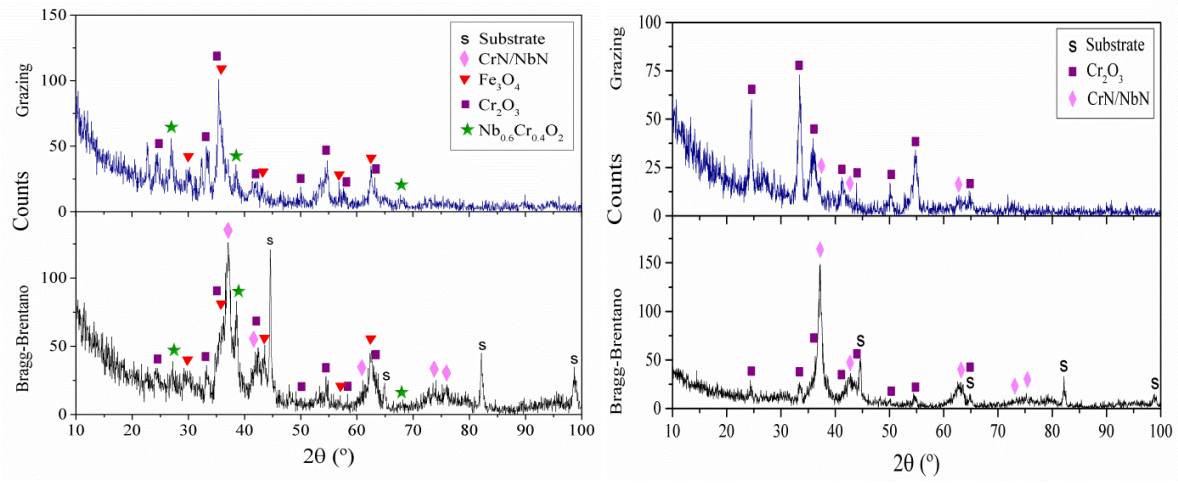

(b) (c)

FIGURE 9. XRD analysis of oxidized coatings at 650ºC in 100% steam atmosphere, after 2000 h: (a) low Nb-CrN/NbN #46, (b) high Nb-CrN/NbN #46 and (c) CrN/NbN high Nb #1000.

CONCLUSIONS

Three CrN/NbN multilayer coatings deposited by PVD-HIPIMS on P92 steel have been evaluated in 100% steam atmosphere at 650ºC. Thermogravimetric studies have shown that the three studied coatings have improved the corrosion resistance of the P92 steel employed as substrate in several orders of magnitude. Furthermore, SEM-EDX and XRD analysis have revealed the presence of intact CrN/NbN coating (irrespective of the Nb content) and of Fe-rich oxides on the surface of those coatings with a coarse substrate surface finishing. Discontinuities formed due to rough substrate surface and contamination related defects are believed to be the reason for interdiffusion of Fe from the substrate. In contrast, the coatings with a fine substrate surface finishing developed a protective layer of chromia on the coating surface that hindered the ionic diffusion of Fe completely. Consequently, as the surface preparation of the base material is crucial to any PVD deposition technique, it also played a defining role in the HIPIMS deposited coatings in this study.

ACKNOWLEDGMENTS

The research for this work was financially supported by the European Commission (Project within FP7-NMP, "Production of Coatings for New Efficient Clean Coal Power Plant Materials", POEMA, grant agreement 310436). The authors gratefully acknowledge the intellectual efforts of all partners.

REFERENCES

1. D. H. Allen, J. E. Oakey and B. Scarlin, in *Materials for Advanced Power Engineering, Part III, Proceedings International Conference*, Liege (1998).
2. P. J. Ennis and A. Czyrska-Filemonowicz, *Sādhanā* **28**, 709 (2003).
3. P. J. Ennis and W. J. Quadakkers, *International Journal of Pressure Vessels and Piping* **84**, 82 (2007).
4. K. Jin, S. Qiu, R. Tang, Q. Zhang and L. Zhang, *Journal of Supercritical Fluid*s **50**, 235 (2009).
5. V. Rohr, M. Schütze, E. Fortuna, D. N. Tsipas, A. Milewska and F. J. Pérez, *Materials and Corrosion* **56**, 874 (2005).
6. Y. Zhang, A. P. Liu and B. A. Pint, *Materials and Corrosion* **58**, 751 (2007).
7. S. Velraj, Y. Zhang, E. W. Hawkins and B. Pint, *Materials and Corrosion* **63**, 909 (2012).
8. B. Navinšek, P. Panjan and I. Milošev, *Surface and Coating Technology* **97**, 182 (1997).
9. J. Lin, N. Zhang, W. D. Sproul and J. J. Moore, *Surface and Coatings Technology* **206**, 3283 (2012).
10. J. C. Sánchez-López, D. Martínez-Martínez, C. López-Cartes, A. Fernández, M. Brizuela, A. García-Luis and J. I. Oñate, *Journal of Vacuum Science & Technology A* **23**, 681 (2005).
11. T. C. Rojas, S. El Mrabet, S. Domínguez-Meister, M. Brizuela, A. García-Luis and J. C. Sánchez-López, *Surface and Coating Technology* **211**, 104 (2012)
12. S. Mato, G. Alcalá, M. Brizuela, R. Escobar-Galindo, F. J. Pérez and J. C. Sánchez-López, *Corrosion Science* **80**, 453 (2014).
13. M. Stueber, H. Holleck, H. Leiste, K. Seemann, S. Ulrich and C. Ziebert, *Journal of Alloys and Compounds* **483**, 321 (2009)
14. B. Borawski, J. Singh, J. A. Todd and D. E. Wolfe, *Wear* **271**, 2782 (2011).
15. A. Inspektor and P. A. Salvador, S*urface and Coatings Technology* **257**, 138 (2014).
16. P. Eh. Hovsepian, D. B. Lewis, W. D. Münz, S.B. Lyon and M. Tomlinson, *Surface and Coating Technology* **120**, 535 (1999).
17. G. L. Miller, *Tantalum and Niobium*, (Butterworths Scientific Publications, London, 1958).
18. M. M. Stack, Y. Purandare and P. Eh. Hovsepian, *Surface and Coatings Technology* **188**, 556 (2004).
19. P. Eh. Hovsepian, D. B. Lewis, Q. Luo and A. Farinotti, *Thin Solid Films* **488**, 1 (2005).
20. H. W. Wang, M. M. Stack, S. B. Lyon, P. Eh. Hovsepian and W. D. Münz, *Surface and Coatings Technology* **126**, 279 (2000).
21. A.P. Ehiasarian, P. Eh. Hovsepain, L. Hultman and U. Helmersson, *Thin Solid Films* **457**, 270 (2004).
22. C. Reinhard, A. P. Ehiasarian and P. Eh. Hovsepian, *Thin Solid Films* **515**, 3685 (2007).
23. Y. P. Purandare, A. P. Ehiasarian and P. Eh. Hovsepian, *Journal of Vacuum Science & Technology A* **26**, (2), 288 (2008).
24. P. E. Hovsepian, D.B. Lewis, W.-D. Munz, A. Rouzaud and P. Juliet, *Surface & Coatings Technology **116–119***, 727 (1999).

25. R. Smith, *Journal of the Less Common Metals* **2**, 191 (1960).
26. O. Kubaschewski and B. E. Hopkins, *Journal of the Less Common Metals* **2**, 172 (1960).
27. W. M. M. Huijbregts and M. J. Brabers, in *Journee internationales d'étude sur l'óxydation des metaux, Proceedings S.E.R.A.I.*, Brussels (1965).
28. W. Wei, H. Wang, C. Zou, Z. Zhu and Z. Wei, *Materials and Design* **46**, 1 (2013).
29. Y. P. Purandare, A. P. Ehiasarian, M. M. Stack and P. Eh. Hovsepian, *Surface and Coating Technology* **204**, 1158 (2010).
30. P. Eh. Hovsepian, A. P. Ehiasarian, Y. P. Purandare, B. Biswas, F. J. Pérez, M. I. Lasanta, M. T. de Miguel, A. Illana, M. Juez-Lorenzo, R. Muelas and A. Agüero, *Materials Chemistry and Physics* **179**, 110 (2016).